ISAS - INTERNATIONAL SCHOOL
FOR ADVANCED STUDIES

Molecular dynamics study of a potassium channel

Thesis submitted for the degree of

"Magister Philosophiæ"

CANDIDATE

Leonardo Guidoni

SUPERVISORS

Dott. Paolo Carloni

Prof. Vincent Torre

October 1998

SISSA - SCUOLA
INTERNAZIONALE
SUPERIORE
STUDI AVANZATI

TRIESTE
Via Beirut 2-4

TRIESTE

SISSA ISAS
SCUOLA INTERNAZIONALE SUPERIORE DI STUDI AVANZATI
INTERNATIONAL SCHOOL FOR ADVANCED STUDIES

Molecular dynamics study of a potassium channel

Thesis submitted for the degree of

"Magister Philosophiæ"

CANDIDATE

Leonardo Guidoni

SUPERVISORS

Dott. Paolo Carloni

Prof. Vincent Torre

October 1998

Contents

Chapter 1

Introduction

The recent developments in molecular biology, crystallization techniques and biophysics have opened new avenues for understanding the molecular basis of biological mechanisms. On the other hand, the increasing computational power and the numerical technique development is allowing the application of theoretical approaches such as classical Molecular Dynamics (MD) simulations to larger and larger biomolecules. By these simulations it is now possible to get structural and dynamical data which may be compared with biological experiments.

In this work we investigate some aspects of ionic channels, comparing our findings with electro-physiological and site directed mutagenesis data. Ionic channels are membrane proteins allowing cells to exchange anions and cations with the extracellular environment. These processes are involved in many biological functions such as nervous signal transmission and osmotic regulation. The recent solution by X-ray of the structure of a bacterial K^+ channel (KcsA) has opened a new avenue for understanding the energetics of fundamental processes such as permeation, ion binding and selectivity [1].

We have performed classical Molecular Dynamics simulations on the complex KcsA channel [1], water and n-octane interfaces with Na^+ and K^+ in different initial positions. We used "all atom" AMBER force field [2] and periodic boundary condi-

tions with the Particle Mesh Ewald method for treating the electrostatic interactions. During the 2 ns dynamics, salt bridges between Asp-80 and Arg-89 of neighboring sub-units, not evident in the X-ray structure, enhanced the stability of the tetrameric structure. This feature may be common to other similar proteins as suggested by sequence alignment of other potassium channels present in nature. Simulation carried out on the R89C mutant further reveal the functional role of these two residues: both the selectivity filter region and the center of mass of the four subunits drift away from the starting position, indicating an overall instability of the quaternary structure. Our findings are completely consistent with site directed mutagenesis experiments in 80 and 89 positions, which essentially abolished protein expression [3] . The binding of metals to the protein was studied by locating hydrated K^+ and Na^+ ions in the outer vestibule. These cations lost part of their hydration shell and diffused into the channel inner pore in less than hundred ps. This powerful catalytic action was caused by the electrostatic potential shape in the vestibule of the channel, mainly due to Asp-80 and Glu-71 interactions.

In the second chapter we summarize some aspects of the biological problem. We insert the studied system in a larger context, and then we will describe the crystal structure. A good knowledge of the three-dimensional structure is necessary for understanding the whole simulation. The third chapter is devoted to the description of the simulation details, focusing on the building of the hydrophobic/hydrophilic environment and the making up of the starting structure. Results are reported in the fourth chapter. The first section reports some general structural features of the simulations. In the second section we compare two different simulations performed on the wild type and on the R89C mutant as stated above. The binding of metals to the proteins is described in the third section. There, we compare electrostatic calculations with MD simulations in order to investigate the catalysis of the dehydration process. Finally, we summarize the results in the fifth chapter.

Chapter 2

Biophysical introduction

2.1 Ionic channels

The purpose of this section is to provide a very short biophysical introduction to ionic channels. Like any other protein, ionic channels are built by a sequence of amino-acids linked together and folded in the native three-dimensional structure [4, 5]. These proteins are macromolecular pores in cell membranes, allowing cells to exchange anions and cations with the extracellular environment (see Fig. 2.1) [5]. Evolution built a membrane around the earliest form of life in order to isolate it from the external environment. The cell membrane is constituted by two layer of phospholipids, which are molecules having a polar head and non-polar tails. Two films of these molecules are assembled together by hydrophobic forces building a very stable lipid bilayer. The presence of the membrane prevents access to necessary ionized substrates and ions, because the hydrophobic core is a high free energy barrier in the diffusion of charged molecules. Ionic channels, inserted in the membrane lipid bilayer as shown in Fig. 2.1, allow ions to cross the hydrophobic region by forming aqueous pores through the membranes. The ionic fluxes produce detectable electric currents and changes of the membrane electric potential. These processes are involved in many biological functions such as nervous signal transmission and osmotic regulation [6].

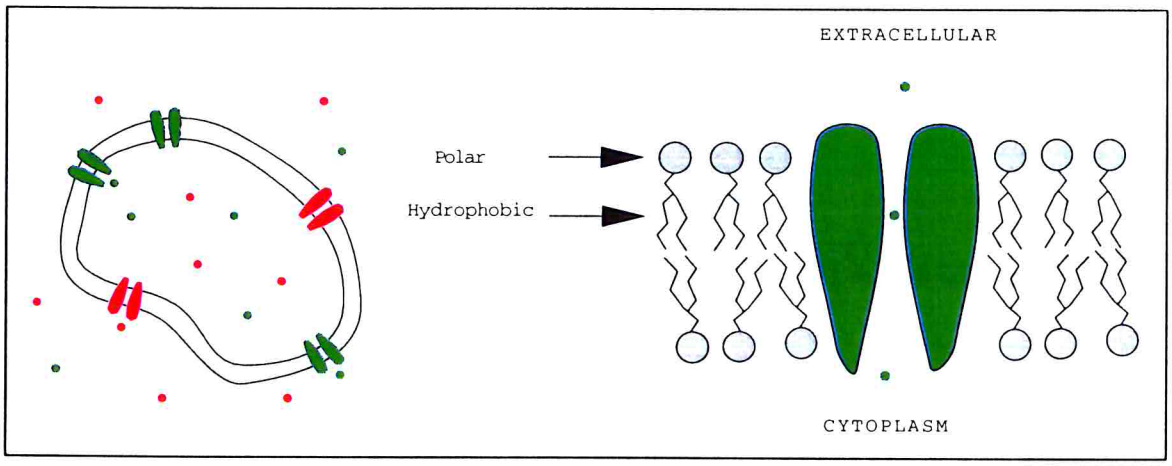

Figure 2.1: Ionic channels in cells. The left drawing represents a membrane cell in which ionic channels are inserted and ions are allowed to flow from one side to the other. Different ionic channels may be present in the same cell, each one selective to a class of ions (dots). The right drawing represents the membrane insertion of the channel protein in the phospholipid bilayer.

Different kinds of ionic channels are present in nature, differing in functional, gating and selectivity properties. The open state of the channel pore may be regulated by physical factors, such as voltage gated channels [7], or by chemical factors such as the presence of ligand molecules (i.e. cyclic nucleotide activated channels [8]) or pH variations (i.e. KcsA potassium channel [9, 3, 10]). Ionic channels are often selective for some ionic species over others. The channel we studied is from a prokariotic cell, the *Streptomyces lividans* (KcsA channel). It is selective for K^+ over Na^+, similar to usual K^+ channels [6]. The selectivity ratio between Na^+ and K^+ $\frac{P_{Na+}}{P_{K+}}$ based on the reversal potential in biionic conditions is less than 0.07 in potassium channels [6]. This ratio in the KcsA channel is 0.35 [9] (see also ref. [10]).

2.2 The crystal structure

The KcsA potassium channel is formed by four identical subunits, each composed of 158 residues, among which 97 are detected in the crystallographic structure. The crystal structure is shown in Fig. 2.2. In the upper left panel the full structure is represented by sticks. Every subunits contains three α helices: two transmembrane helices which cross the cell membrane, and one shorter helix near the pore of the channel. Two rings of aromatic residues characterize the membrane/water interfaces (namely Trp-26 and Trp-113 in the cytoplasmic side, Trp-67 and Trp-87 in the extracellular side), as often happens in integral membrane proteins. The tetrameric structure of the protein is emphasized by using different colors for the four subunits as in the upper right panel, where helices are represented by cylinders. Three binding sites for the potassium atoms were identified, in agreement with the traditional view that K^+ channels are multi-ion channels [11, 12, 13] (green spheres in Fig. 2.2). A crystallographic water molecule has also been detected between the two more external (i.e. extracellular) potassium ions (red sphere in Fig. 2.2. The selectivity filter, located between the first and second binding site, is a narrow funnel with a diameter of 3 Å , lined with backbone carbonylic oxygens [14]. This region was identified by sequence alignment (Fig. 4.3) and mutagenesis experiments as the fingerprint of the potassium channels family, responsible for the K^+ selectivity. The potassium ions inside the selectivity filter are bounded by backbone carbonylic oxygens belonging to the all four chains as is shown by the lower panels in Fig. 2.2. In this way protein oxygens replace the K^+ hydration shell in the bulk water, compensating for the loss in energy due to the ion dehydration. We discuss some aspects of the alkali binding in the results chapter.

The Debye-Waller factors of the crystal structure at 3.2 Å resolution are quite large (backbone average 90 ± 38 Å^2), reflecting the difficulties in obtaining high quality crystals from integral membrane proteins.

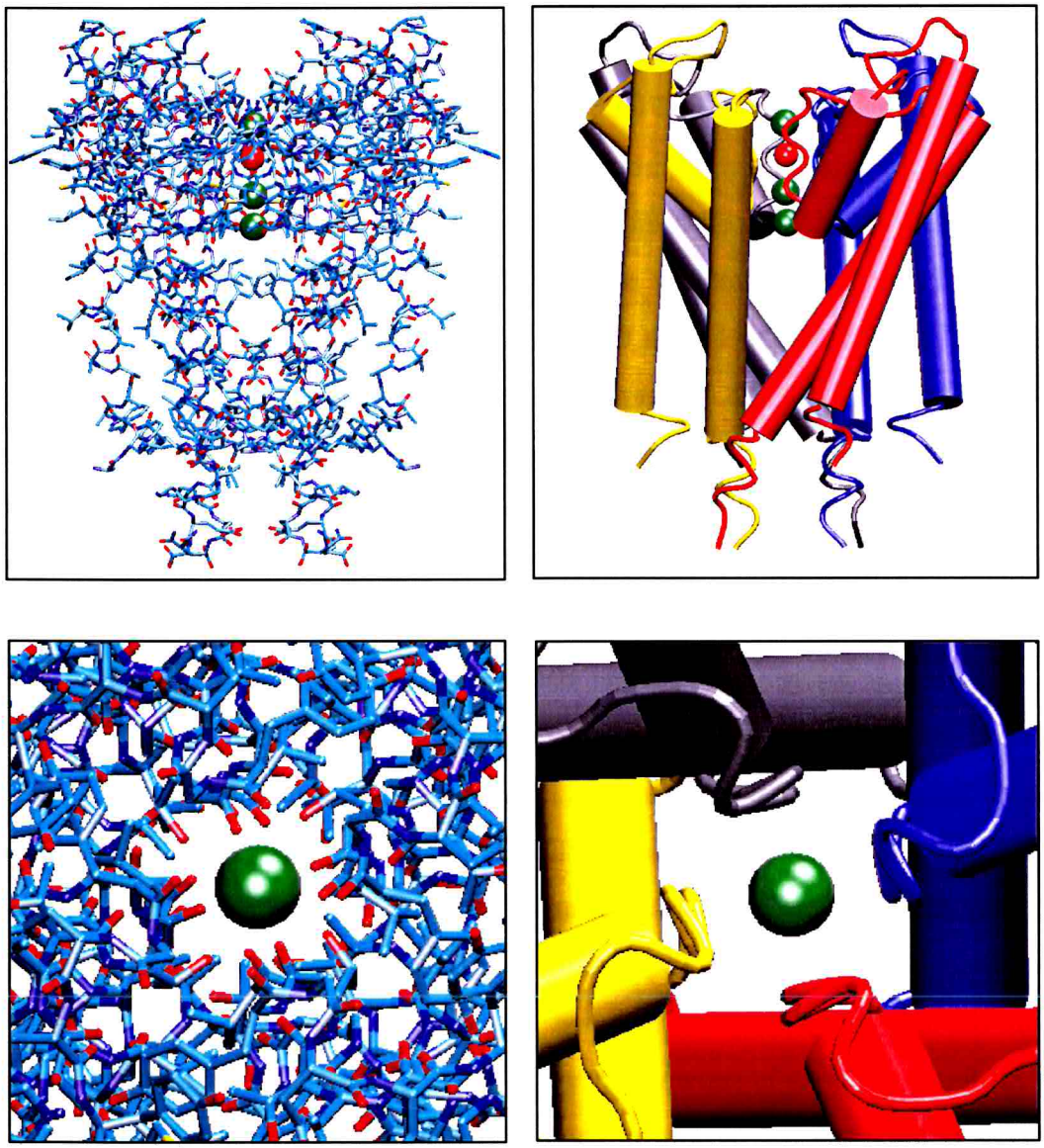

Figure 2.2: The crystallographic structure of KcsA from *Streptomyces lividans* [1]. In the upper panel the full structure is drawn in sticks (left) and schematic (right) representations. The lower panels magnify the top view of the selectivity filter region. Further details are discussed in the text.

Chapter 3

The simulations

3.1 The starting structure

Our structural model is based on the structure of the KcsA potassium channel described in the previous chapter [1]. Part of the side chains of 5 amino acids (Arg-27, Ile-60, Arg-64, Glu-71, Arg-117) missing in the X-ray structure were added using standard residues geometries, taking care to avoid unphysical contacts. The only histidine present in the protein (His-25) was assumed to be protonated in the δ position, as N_δ forms an H-bond to the carbonyl group of Ala-109. The missing atoms of the Glu-71 side chains were added so as to point towards the NH groups of the Tyr-78 backbone [15].

The cytoplasm/membrane environment was mimicked by a water/n-octane bilayer enclosed in a box [16]. This approach supplies a stable hydrophilic/hydrophobic liquid interface quickly adaptable to protein geometry, avoiding the stiffness of full phospholipids. The portion of the protein immersed in the organic liquid is comprised between two layers of aromatic residues, 34 Å from each other, believed to point toward the two putative membrane/water interfaces [1]. Thus, we have immersed this region of the protein between the two layers (namely between Tyr-62 and Phe-114) in the n-octane solution. The computational scheme used to construct the water/n-

octane/water layers as well as the procedure of immersing the protein into the solvent are given in next paragraph.

The positive charge of the protein was neutralized by leaving the C- terminal tail of each chain deprotonated and the N-terminal tail uncharged. Cl^- counterions where added close to Arg-117 to balance the charge of added K^+ or Na^+ ions.

3.2 Computational details

In this section the parameters, the force field and the procedures used in our MD simulations will be discussed. All the simulations were carried out with periodic boundary conditions, constant temperature and constant volume. We used the AMBER 5 suite of programs [17]. The temperature was maintained at 298K with the Berensden's thermal coupling [18] using a 0.2 ps separate relaxation time for solvent and solute. The Coulomb interaction was treated using the particle mesh Ewald [19] method with $\sim$ 1 Å in charge grid spacing interpolated by 3rd order B-spline and by setting the direct sum tolerance to $5 \cdot 10^{-6}$. We have used a 8 Å cutoff for the nonbonded short-ranged interactions. The SHAKE algorithm [20] has been used to constrain all bonds. A time step of 1 ps was used. The all-atom AMBER force field [2, 21] and the OPLS force field [22, 23] were used for the protein, the alkali metal ions and n-octane respectively. The water model was the TIP3P [24]. To obtain a structural model of the water/n-octane/water interfaces we considered a box of dimensions $a \times b \times c = (65 \times 66 \times 69\ )$ Å^3 and periodic boundary conditions, then we positioned two slabs of water and octane (respectively 35 and 34 Å in thickness) on the ab plane. The densities of both liquids was adjusted in the starting configuration to the experimental values. We carried out an NVT-MD run on this system for more than 500 ps. During this time the bilayer has shown a very high stability and the ability to totally drive water out of the hydrophobic region as shown in Fig. 3.1. The final structure obtained has sharp and well defined hydrophobic/hydrophilic interfaces where the KcsA starting structure will be located.

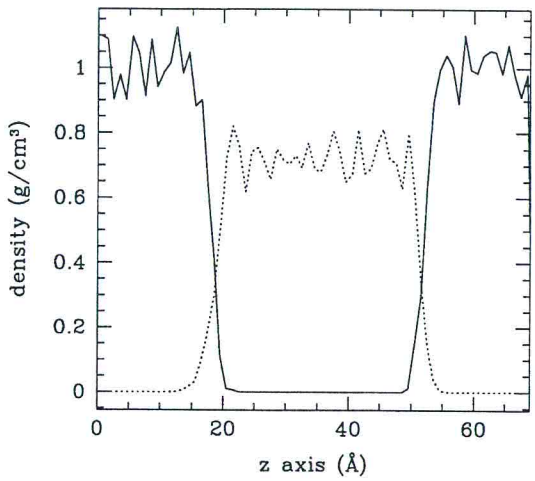

Figure 3.1: Density profiles of n-octane (dotted line) and water (solid line) along the channel symmetry axis show how the two slabs are well separated. Analogous simulations based on United-Atoms force field [16] allowed the permeation of some water molecules inside the core of the membrane. This non biological situation is avoided using an All-Atom force field.

Although inserting a channel protein in a membrane had always presented some difficulties, our model membrane allowed us to use a simple procedure. We estimated the volume of the protein in the hydrophobic and hydrophilic regions by calculating the Connolly surfaces [25] in the two regions. We then eliminated water and octane molecule consistently with the calculated volumes and with the bulk experimental densities. Finally, we located the crystallographic water molecule and 29 other water molecules into the channel pore by calculating again the internal Connolly volume. To equilibrate the solvent around the protein, we used the following prôcedure: i) 40 ps of MD for the water molecules keeping the protein and the n-octane fixed; ii) 40 ps of MD keeping the rest fixed; iii) full relaxation of the water and n-octane solvent for another 200 ps of MD.

Several MD simulations of the protein, its R89C mutant, and complex with K^+ and Na^+ ions were performed: i) K^+- protein complex (K^+ located in the first binding site); ii) K^+ (or Na^+) located in the external mouth: the position was first constrained

at 6 Å from the binding site during thermalization; iii) same as ii) but without constraint; iv) same as iii) but with another K^+ at 6 Å from the second binding site and starting from the last snapshot of i); v) K^+- R89C mutant complex (K^+ located in the first binding site). Simulation times were: i) 1.5 ns, ii)-iv) 0.3 ns; v): 0.7 ns, of which 0.12 ns were used for heating the systems from 0 to 298 K. All the structural models exhibited a good Ramachandran plot with no residues in outlying regions.

Chapter 4

Results

4.1 General structural properties

During the dynamics, the structure of the channel-K^+ complex (Fig. 4.2A) was stable: as shown in Fig. 4.1, after 0.5 ns, and for the rest of the simulation (up to 1.5 ns) atoms of the protein backbone fluctuated with a root mean square displacement (rms) with respect to the starting structure of 2.3 ± 0.1 Å. Residues forming the turret (from 52 to 61) experienced fluctuations larger than those lining the selectivity filter (residues 75-79) (Fig. 4.2B). The relatively high stability of the selectivity filter may be an important physical mechanism for ionic selectivity [26]. The secondary structure of the 12 α-helices remained stable throughout the simulation, with the hydrogen bonds along each backbone well maintained. The starting position of the K^+ turned out not to be stable since the thermalization run at 20 K. The ion quickly occupied the crystallographic water position, about 4 Å away from the starting point in the inner direction, and remained there for the remainder of the simulation. Probably this instability is due to the different binding sites of the channel when the selectivity filter is occupied by one ion instead of two (as in the X-ray structure). A simulation in the absence of a K^+ ion in the binding site also underlined the important role of the metal ion for protein stability. Indeed, the selectivity filter region backbone (from Tyr-75

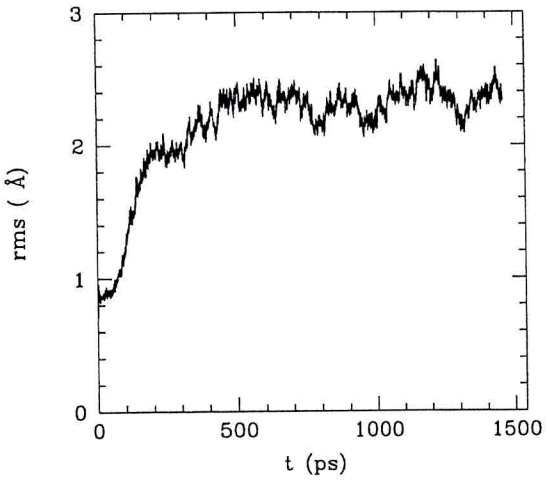

Figure 4.1: The backbone atoms rms. A little slope appears after 0.5 ns. The rms is calculated by fitting the the evolved structure with the minimized one.

to Gly-79) of the KcsA channel, without a K^+ inside, experienced larger mobility than that of the KcsA channel with a K^+ ion in the inner pore (rms fluctuations were (1.9 ± 0.5) Å and (1.0 ± 0.3) Å respectively).

4.2 Mutagenesis analysis

The quaternary structure of the channel was stabilized by the formation of salt bridges between the Arg89 and Asp80 of neighboring subunits (Fig. 4.2C), not evident in the X-ray structure. These salt bridges broke and formed on the ns time scale (Fig. 4.2D). Force-field based calculations show that these salt bridges are very important for the integrity of the quaternary structure, as they account for about half of the total subunit-subunit association energy. The proposed role of these two residues agrees with the observation of the structural similarity of the KcsA channel and prokaryotic K^+ channels [27] and with the conservation of these residues in a variety of K^+ channels. A sequence alignment of eukaryotic and prokaryotic proteins belonging to the K^+ channels family reveals that Asp-80 and Arg-89 (or Lys-89) are a pair of conserved residues in the pore region. As Fig. 4.3 shows, these two residues are simultaneously

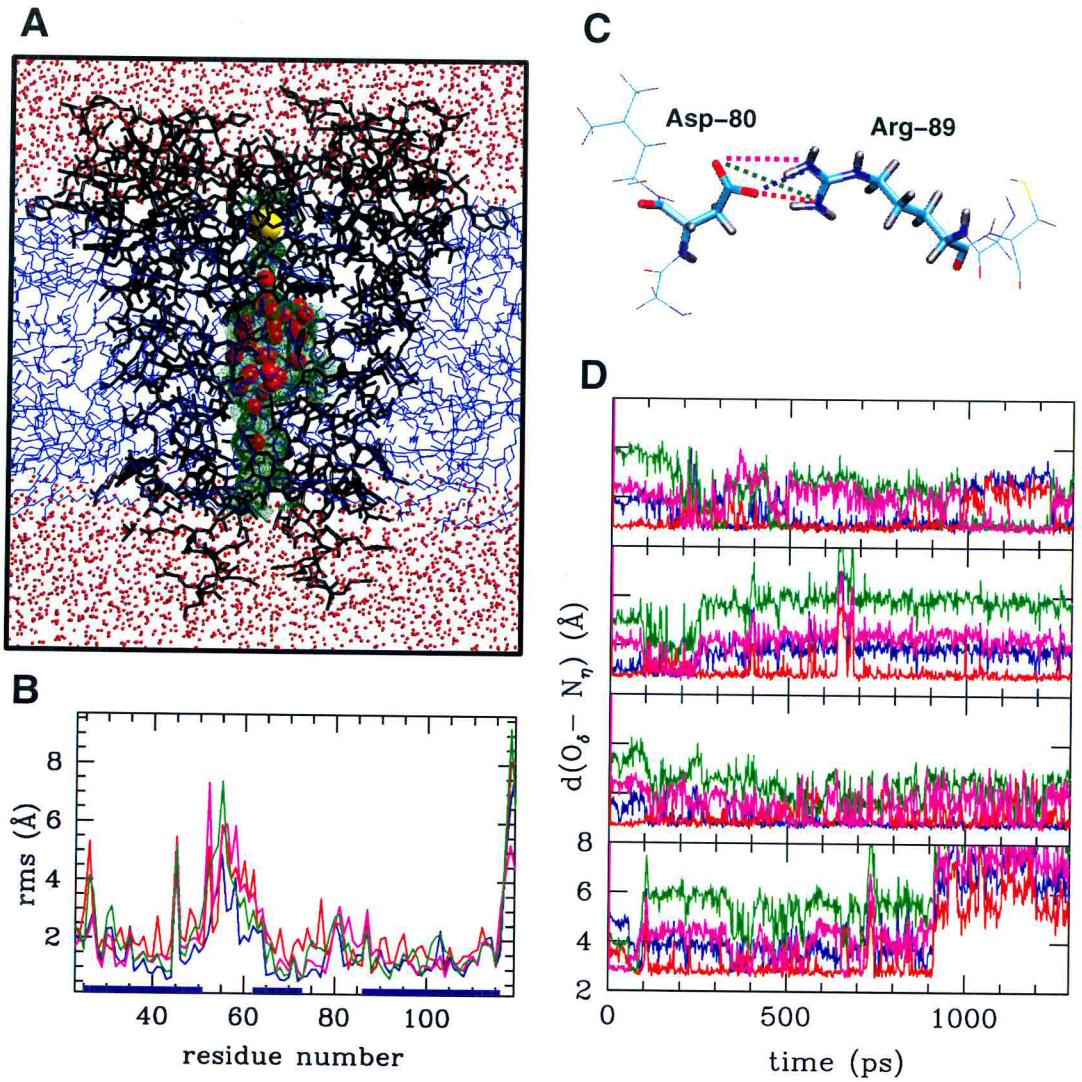

Figure 4.2: Molecular dynamics on the protein-K^+ complex. (A) The protein is immersed in an octane-water bilayer (blue and red, respectively) with a potassium ion (in yellow). The Connolly surface [25] within the channel pore is in green. (B) rms fluctuations per residue from the protein starting structure. The four colors (magenta, green, red and blue) refer to the four subunits, while the blue bars on the abscissae indicate the inner (residues 25 to 51), the pore (62 to 73) and outer (86 to 116) helices. (C) View of the Asp80-Arg89 salt bridge and (D) corresponding carboxylate oxygen-guanidinium nitrogen distances plotted as a function of time. Distances are plotted for the four Asp-80–Arg-89 pairs.

conserved in 11 sequences; further sequences are aligned in ref. [28]. To further explore the Asp80-Arg89 induced subunit-subunit stabilization, a simulation where Arg89 was mutated into a cysteine (R89C mutant) was carried out, mimicking the experiment of E. Perozo *et al.* [3], in which this mutation essentially abolished protein expression in KcsA channel (11). After a few hundred ps, the quaternary structure of the mutant lost its original conformation (Fig. 4.4) and the selectivity filter became wider (Fig. 4.4B). Actually, analogous mutations in other K^+ channels revealed a similar loss of functional expression: D378T and D378C in *Kv2.1* [29, 30], K456D in *Shaker* [31]. Our calculations thus suggest that the loss of functional expression of K^+ channels where the aspartate and/or the arginine (or lysine) near the external vestibule were mutated [3, 29, 30] was due to a partial disruption of the quaternary structure and of the selectivity filter.

4.3 Alkali binding

The electrostatic potential energy of the protein, calculated with the Poisson- Boltzmann equation (12), was significantly negative in the channel vestibule and close to the first binding site (Fig. 4.5A). The energy profile turned out to be very similar in the presence or absence of a K^+ ion in the second binding site. Thus the KcsA channel attracts cations and repels anions from its inner pore. This valence selectivity was largely caused by the external ring of Asp-80 and the more internal ring of Glu-71 (Fig. 4.5B). The ring of positively charged Arg-89 (Fig. 4.5B), located more distant from the channel axis, balanced but not abolished the attraction of cations . When a potassium ion was in the first binding site the electrostatic potential energy in the channel vestibule was less negative. The binding of metals to the protein was studied by locating hydrated K^+ or Na^+ ions in the outer vestibule. Simulations carried out with and without the potassium in the second binding site lead to very similar results. At the beginning of the simulations ions were located in the bulk solvent (at 6 Å from the pore region) and were coordinated by six (Na^+) or eight

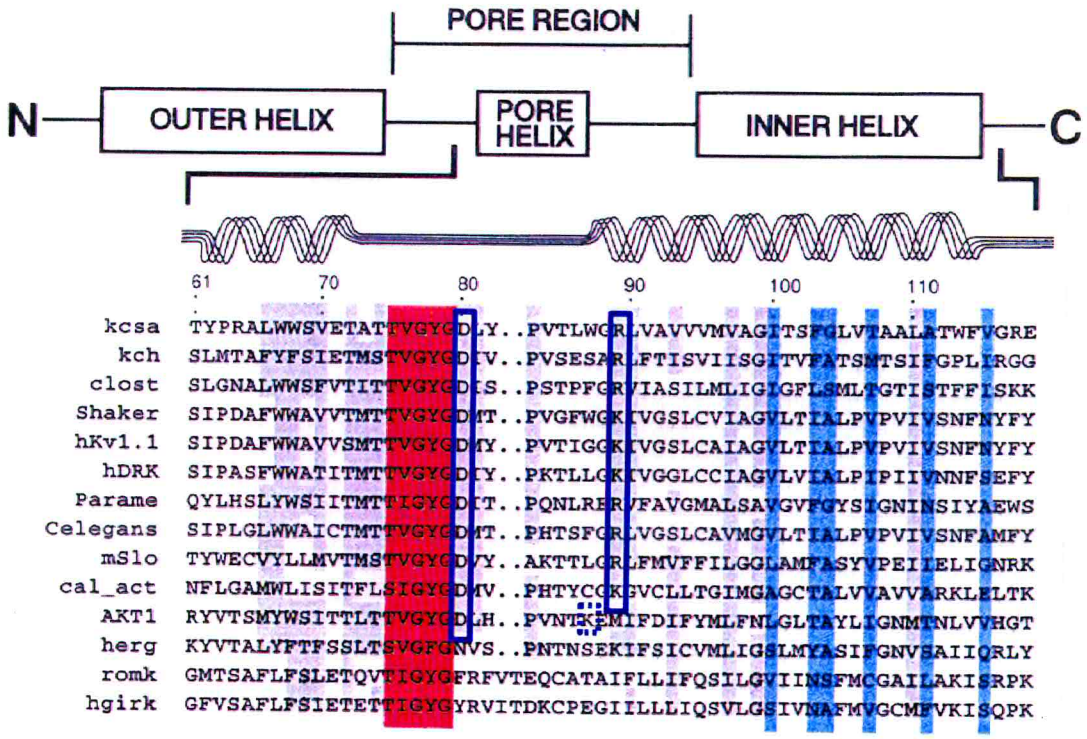

Figure 4.3: Alignment of K^+ channel sequences. The red filled box is the selectivity filter, responsible for K^+ selectivity. The blue boxes emphasize the conserved position of the pair Asp-80/Arg-89(Lys-89) which we suppose to be involved in intrachain salt bridges. The sequences for aspartic acid and arginine are (from top to bottom): Streptomyces lividans (PIR S60172); Escherichia Coli (GenBank U24203); Clostridium acetobutylicum (Genome Therapeutics Corp.); Paramecium tetraaurelia (GenBank U19908); Caenorhabditis elegans (GenBank AF005246); Mus musculus (PIR A48206). The sequences for aspartic acid and lysine are: Shaker, Drosophila melanogaster (PIR S00479); Homo sapiens (Swissprot Q09470); Homo sapiens (PIR S31761); Homo sapiens (GenBank AF031815). The figure is modified from ref [1].

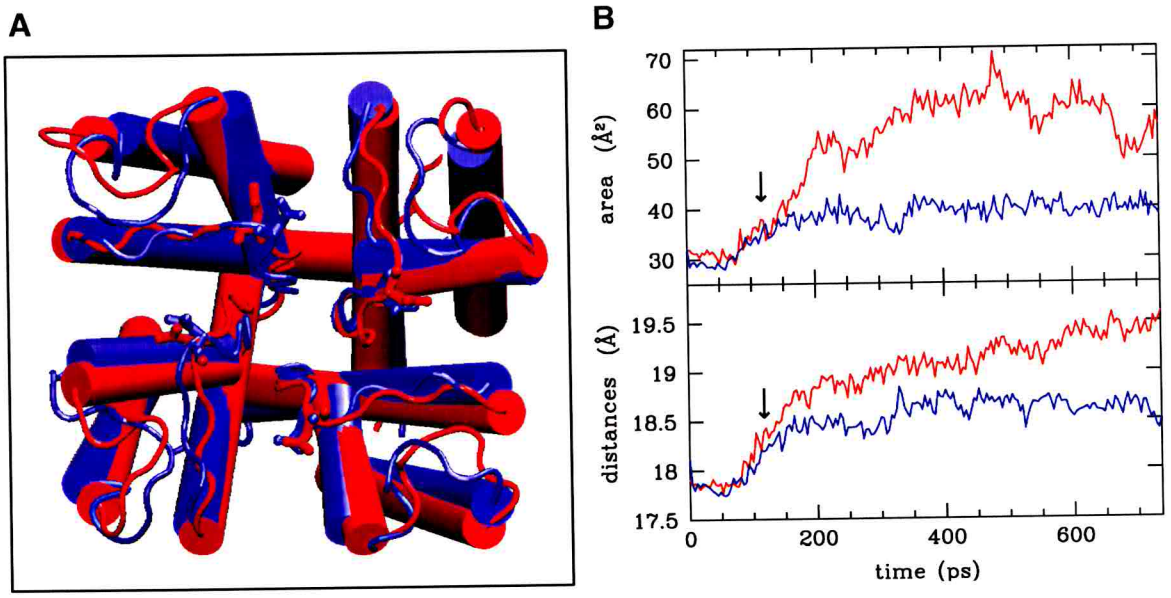

Figure 4.4: Molecular dynamics of the KcsA (blue) and of its R89C mutant (red). (A) Comparison between the two structures after 450 ps (α helices indicated as cylinders). (B) Selected geometrical features as a function of time. Bottom: average distances between the center of mass of the four subunits. Top: pore area of the four subunit pore walls (residues from 76 to 79). The mutant channel exhibits a larger drift than the wild type KcsA channel. The arrow indicates the time when thermalization at 298 K was achieved.

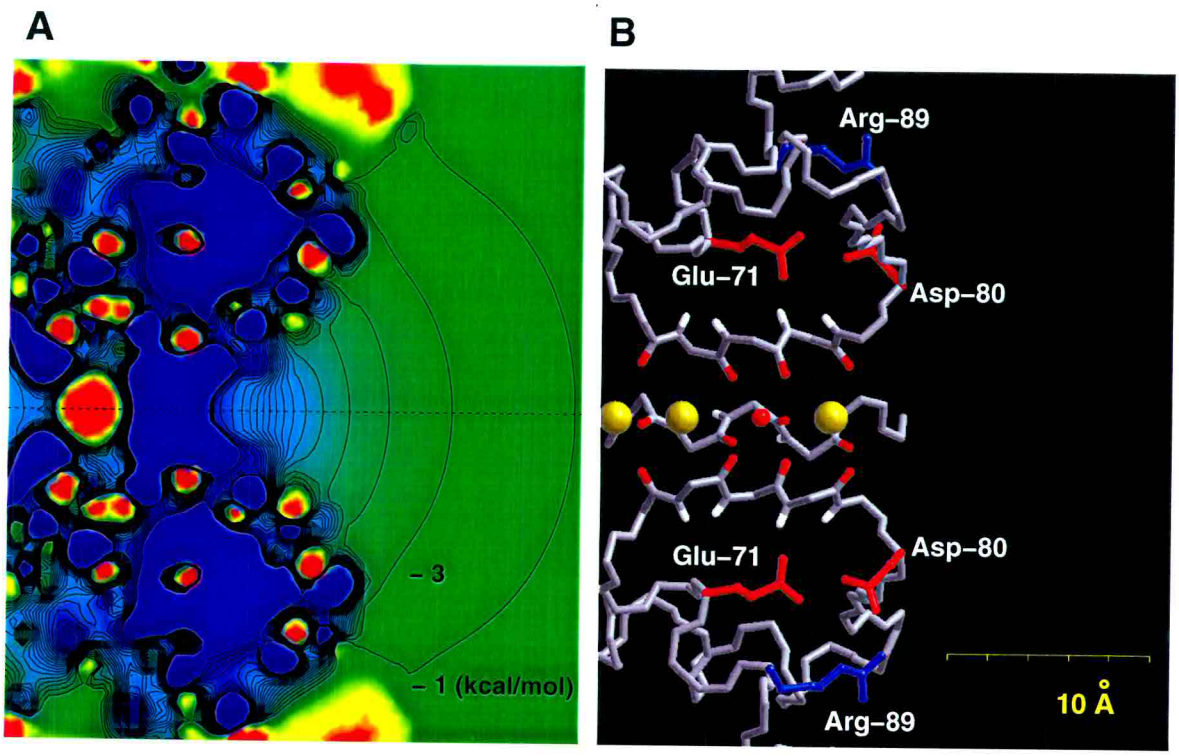

Figure 4.5: Electrostatic energy profile in the outer mouth of the KcsA channel. (A) Electrostatic potential energy [32, 33] in the pore and solvent regions through a planar section containing the channel axis. We used dielectric constant $\epsilon = 78$ for the water and $\epsilon = 2$ for the protein. The initial configuration of the KcsA channel was used with a potassium ion in the second binding site. Black lines indicate isoenergy contours at a 2 kcal/mol separation. Red (blue) indicates a very positive (negative) electrostatic energy and therefore cation repulsion (attraction). (B) The structure of some residues contributing to the electrostatic energy profile in A. The three yellow spheres indicate the three binding sites. The first binding is the more external. The small red sphere is the oxygen of the crystallographic water molecule. Backbone oxygens (red) and the amide hydrogens (white) in the selectivity filter of three subunits. Asp-80 and Glu-71 of two opposing subunits (red) and two Arg-89 of the two other subunits (blue). Diagrams in A and B are on the same scale.

Figure 4.6: Binding of Na^+ and K^+ to the channel. Top: Selected snapshots ((A): after 2 (left), 16 (middle), and 60 (right) ps; (C): after 2 (left), 24 (middle) and 60 (right) ps) are shown for both K^+ (A) and Na^+ (C) cations: ions are completely hydrated in the outer mouth of the vestibule (left), they interact with the protein (middle) and diffuse into the first binding site (right). Coordination numbers (n) of K^+ (B) and Na^+ (D) plotted as a function of time. n is calculated assuming K^+-(Na^+-) ligand cutoff of 3.65(3.25) Å [34]. Total coordination number (solid line) and contributions from the solvent (dashed) and from the backbone (dotted line) are reported.

(K^+) water molecules (first panels of Fig. 4.6 A and C). Both ions diffused within a few tens of ps towards the first binding site (second panels of Fig. 4.6 A and C) and lost part of their hydration shell (Fig. 4.6 B and D). Diffusion occurred in the absence of any external driving force. K^+ was coordinated to two water molecules and to the backbone carbonylic oxygen atoms of Gly-77 and Val-76 (last panel of Fig. 4.6A). Na^+ was coordinated to three water molecules and to the backbone oxygens of Gly-77 and Tyr-78 (last panel of Fig. 4.6C). Thus potassium was coordinated to less water molecules than sodium and entered more deep into the channel inner pore. This different behavior seems a basic feature of the permeation of Na^+ and K^+. As the selectivity filter has larger fluctuations in the absence of K^+ in its inner pore, the exact number of water molecules coordinated to the ions depended on the time during which the inner pore remained empty. For instance, if the latter was larger than 200 ps, K^+ entered the channel inner pore with three and even four water molecules. The different hydration states of Na^+ and K^+ in the channel inner pore seems to be a basic factor determining ionic selectivity (7).

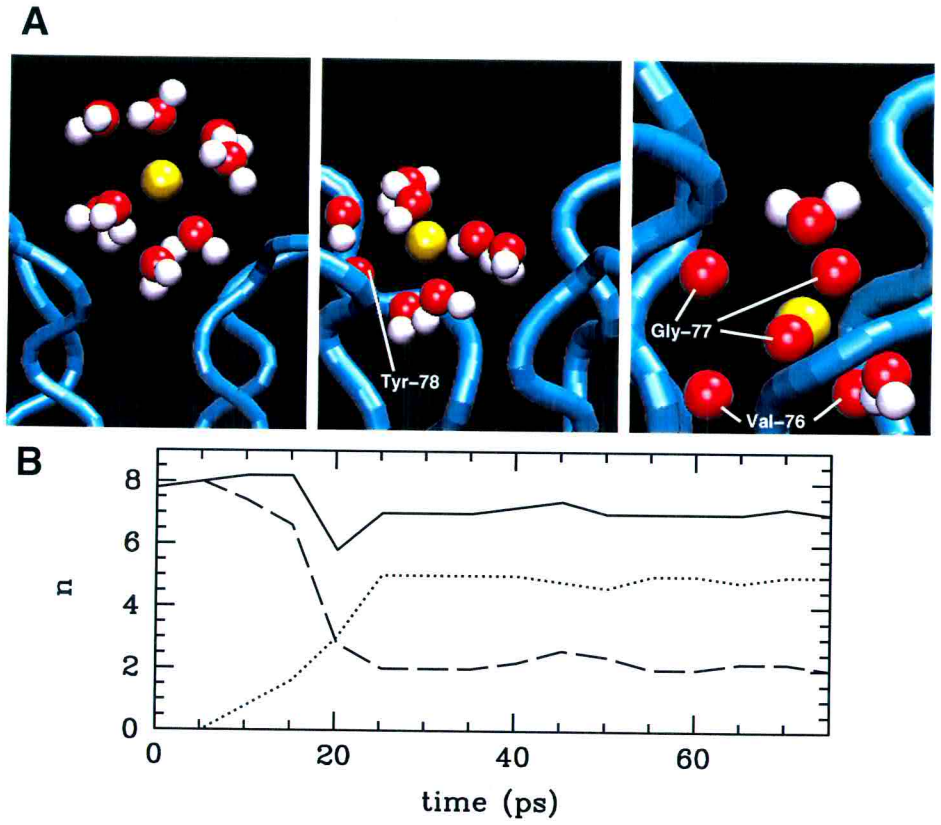
A
Tyr–78
Gly–77
Val–76
B
n
time (ps)
C
Tyr–78
Tyr–78
Gly–77
D
n
time (ps)

Chapter 5

Conclusion

From these simulations several conclusions can be drawn on structural and functional aspects of ion permeation through the KcsA channel. First, the channel is engineered so as to repel anions and attract cations, i.e. K^+ and Na^+, into the first binding site within the pore (Fig. 4.5A). This valence selectivity in an electrically neutral channel is achieved by the specific channel geometry, with negative charges located near to the channel axis (Fig. 4.5B). Second, when the channel is not yet occupied by a cation, the charge configuration of the KcsA channel is able also to strip most of the water molecules from an hydrated cation (Fig. 4.6), thus efficiently catalyzing dehydration. As a consequence, the rate limiting process requiring thermal activation is the removal of the permeating cation from the binding sites. Third, a major difference between Na^+ and K^+ in the channel pore is that Na^+ keeps more water molecules attached to it than K^+. Finally these simulations reveal a novel role for Asp-80, usually thought to be an external binding site: Asp-80 appears to form salt bridges with Arg-89 and therefore contributing to the stability of the tetrameric complex.

Chapter 6

Acknowledgment

First of all I wish to thank Silvia for her enthusiasm about the living world and for having encouraged and helped me in times of trouble.

I gratefully thank my supervisors, Paolo Carloni and Vincent Torre, who introduced me to theoretical and experimental biochemistry and biophysics.

I wish to thank Roderick MacKinnon for providing us with the coordinates of the KcsA channel before the PDB deposition; Frank Alber for his help on DELPHI program; Alessandro Laio and Katia Gamel for helpful discussion; Lorenzo De Santis and Gianni Settanni for comments and suggestions; Poul Tangney for his precious help.

Bibliography

[1] D.A. Doyle, J.M. Cabral, R.A. Pfuetzner, A. Kuo, J.M. Gulbis, S.L. Cohen, B.T. Chain, and R. MacKinnon. The structure of the potassium channel: Molecular basis of k+ conduction and selectivity. *Science*, 280:69–77, 1998.

[2] W.D. Cornell, P. Cieplack, C.I. Bayly, I.R. Gould, K.M. Merz, D.M. Ferguson, D.C. Spellmeyer, T. Fox, J.W. Caldwell, and P.A. Kollmann. A second generation force field for the simulation of proteins, nucleic acids, and organic molecules. *J. Am. Chem. Soc.*, 117:5179–5197, 1995.

[3] E. Perozo, D.M. Cortes, and L. Cuello. Three-dimensional architecture and gating mechanism of a k+ channel studied by epr spettroscopy. *Nature Struct. Biol.*, 5(6):459–469, 1998.

[4] T.E. Creighton93. *Proteins: structure and molecular properties.* W.H. Freeman and Company, New York, 2nd edition, 1993.

[5] L. Stryer. *Biochemistry.* Freeman and Company, New York, 4th edition, 1995.

[6] B. Hille. *Ionic channels of excitable membranes.* Sinauer Associates, Sunderland, Massachusetts, 2nd edition, 1992.

[7] W.A. Catterall. Structure and function of voltage-gated ion channels. *Annu. Rev. Biochem.*, 64:493–531, 1995.

[8] W.N. Zagotta and S.A. Siegelbaum. Structure and function of cyclic nucleotide-gated channels. *Annu. Rev. Neurosci.*, 19:235–263, 1996.

[9] H. Schrempf, O. Schmidt, R. Kummerlen, S. Hinnah, D. Muller, M. Betzler, T. Steinkamp, and R. Wagner. A prokariotic potassium ion channel with two predicted transmembrane segments from streptomyces lividans. *EMBO J.*, 14(21):5170–5178, 1995.

[10] L. Cuello, J.G. Romero, D.M. Cortes, and E. Perozo. ph-dependent gating in the streptomyces lividans k+ channel. *Biochemistry*, 37(10):3229–3236, 1998.

[11] R.D. Hodgkin and R.D. Keynes. The potassium permeability of a giant nerve fibre. *J. Physiol.*, 128:61–88, 1955.

[12] B. Hille and W.J. Schwartz. Potassium channels as multi-ion single-files pores. *J. Gen. Physiol.*, 72:409–442, 1978.

[13] S. Hagiwara and K. Takahashi. The anomalous rectification and cation selectivity of the membrane of a starfish egg cell. *J. Memb. Biol.*, 18:61, 1974.

[14] C. Armstrong. The vision of the pore. *Science*, 280:56–57, 1998.

[15] E. Gouaux. Single potassium ion seek open channel for transmembrane travels: teles from the kcsa structure. *Structure*, 6:1221–1226, 1998.

[16] Q. Zhong, Q. Jiang, P.B. Moore, D.M. Newns, and M.L. Klein. Molecular dynamics simulation of a synthetic ion channel. *Biophys. J.*, 74:3–10, 1998.

[17] D.A. Case, D.A. Pearlman, J.W. Caldwell, T.E. Cheatham III, W.S. Ross, C. Simmerling, T. Darden, K.M. Merz, R.V. Stanton, A. Cheng, J.J. Vincent, M. Crowley, D.M. Ferguson, R. Radmer, G.L. Seibel, U.C. Singh, P. Weiner, and P.A. Kollman. Amber 5, 1995.

[18] H.J.C. Berendsen, J.P.M. Postma, W.F. van Gunsteren, A. DiNola, and J.R. Haak. Molecular dynamics with coupling to an external bath. *J. Chem. Phys.*, 81(8):3684–3690, 1984.

[19] U. Essman, L. Perera, M.L. Berkowitz, T. Darden, H. Lee, and L.G. Pedersen. A smooth particle mesh ewald method. *J. Chem. Phys. B*, 103:8577–8593, 1995.

[20] J.-P. Ryckaert, G. Ciccotti, and H.J.C. Berendsen. Numerical integration of the cartesian equations of motion of a system with constraints: Molecular dynamics of n-alkanes. *J. Comp. Phys.*, 23:327–341, 1977.

[21] J. Aqvist. Ion-water interaction potentials derived from free energy perturbation simulations. *J. Phys. Chem.*, 94:8021–8024, 1990.

[22] G. Kaminski and W.L. Jorgensen. Performance of the amber94, mmff94, and opls-aa force fields for modeling organic liquids. *J. Phys. Chem.*, 100:18010–18013, 1996.

[23] B. Chen, M.G. Martin, and J.I. Siepmann. Thermodynamic properties of the williams, opls-aa, and mmff94 all-atom foce fields for normal alkanes. *J. Phys. Chem. B*, 102:2578–2586, 1998.

[24] W.L. Jorgensen, J. Chandrasekhar, and J.D. Madura. Comparison of simple potential functions for simulating liquid water. *J. Chem. Phys.*, 79(2):926–935, 1983.

[25] M.L. Connolly. Solvent-accessible surfaces of proteins and nucleic acids. *Science*, 221:709–713, 1983.

[26] A. Laio and V. Torre. Physical origin of selectivity in ionic channels of biological membranes. *Biophys. J.*, 76:129–148, 1999.

[27] R. MacKinnon, S.L. Cohen, A. Kuo, A. Lee, and B.T. Chait. Structural conservation in prokaryotic and eukaryotic potassium channels. *Science*, 280:106–109, 1998.

[28] R. Shealy, A. Murphy, R. Ramarathnam, S. Subramaniam, and E. Jakobsson. Bioinformatics of k+ channels. *Biophys. J.*, 76:A190, 1999.

[29] G.E. Kirsch, J.M. Pascual, and C.-C. Shieh. Functional role of conserved aspartate in the external mouth of voltage-gated potassium channels. *Biophysical J.*, 68:1804–1813, 1995.

[30] J.M. Pascual, C.-C. Shieh, G.E. Kirsch, and A.M. Brown. K+ pore structure revealed by reporter cysteines at inner and outer surfaces. *Neuron*, 14:1055–1063, 1995.

[31] S.A.N. Goldstein, D.J. Pheasant, and C. Miller. The charybdotoxin receptor of a shaker k+ channel: peptide and channel residues mediating molecular recognition. *Neuron*, 12:1377–1388, 1994.

[32] B. Honig and A. Nicholls. Classical electrostatic in biology and chemistry. *Science*, 268:1144–1149, 1995.

[33] M.K. Gilson, K.A. Sharp, and B.H. Honig. Calculating the electrostatic potential of molecules in solution: method and error assessment. *J. Comp. Chem.*, 9(4):327–335, 1987.

[34] H.L. Song and C.R. Jayendran. *J. Phys. Chem.*, 100:1420, 1996.